RCR
RADIOLOGY CASE REPORTS

Case Report

Iatrogenic intramuscular hematoma of the oblique muscles as a complication of technetium-99m-labeled pyrophosphate imaging-based computed tomography-guided core-needle biopsy in a patient with wild-type transthyretin cardiac amyloidosis [☆],[☆☆]

Koji Takahashi, MD, PhD[a,b,*], Takaaki Iwamura, MD[c], Yoshiyasu Hiratsuka, MD, PhD[c,1], Daisuke Sasaki, MRT[c], Nobuhisa Yamamura, MLT[d], Mitsuharu Ueda, MD, PhD[e], Mako Yoshino, MD[b], Daijiro Enomoto, MD, PhD[b], Hiroe Morioka, MD[b], Shigeki Uemura, MD[b], Takafumi Okura, MD, PhD[b], Tomoki Sakaue, MD, PhD[a,b], Shuntaro Ikeda, MD, PhD[a,b]

[a] Department of Community Emergency Medicine, Ehime University Graduate School of Medicine, Ehime, Japan
[b] Department of Cardiology, Yawatahama City General Hospital, 1-638, Ohira, Yawatahama, Ehime 796-8502, Japan
[c] Department of Radiology, Yawatahama City General Hospital, Ehime, Japan
[d] Department of Clinical Pathology, Yawatahama City General Hospital, Ehime, Japan
[e] Department of Neurology, Graduate School of Medical Sciences, Kumamoto University, Kumamoto, Japan

ARTICLE INFO

ABSTRACT

Technetium-99m-labeled pyrophosphate imaging-based computed tomography-guided core-needle biopsy of the internal oblique muscle with tracer uptake is a safe and sensitive extracardiac screening biopsy. It can provide histopathological confirmation of the deposition of amyloid transthyretin in patients with wild-type transthyretin cardiac amyloidosis. This case report presents the case of a 73-year-old man receiving triple anti-thrombotic therapy for atrial flutter and coronary stenting who underwent this biopsy to confirm the diagnosis of transthyretin cardiac amyloidosis. The biopsy needle reached the internal oblique

muscle via the external oblique muscle between the skin and the target. A type 1 intramuscular hematoma involving these muscles developed subsequently; however, manual compression hemostasis prevented further increase in size. Since this biopsy often targets elderly patients receiving anti-thrombotic therapy who are at high risk of bleeding owing to multimorbidity and polypharmacy, efforts should be made to reduce the frequency of complications, particularly bleeding, which can lead to the development of intramuscular hematoma.

Introduction

Native transthyretin (TTR) is a homotetrameric protein constituted by 4 fully folded monomers. TTR becomes less stable with age, resulting in its dissociation into partially unfolded and intrinsically amyloidogenic dimeric and monomeric intermediates that ultimately form amyloid TTR (ATTR) deposits, leading to the occurrence of wild-type ATTR (ATTRwt) amyloidosis [1]. Cardiac involvement is a dominant clinical feature observed in almost all cases of ATTRwt amyloidosis. Cardiac amyloidosis is a cardiomyopathy characterized by the accumulation of amyloid fibrils in the interstitial space of all cardiovascular structures, including the atrial and ventricular myocardium, leading to the thickening of the wall and restrictive physiology. Patients with cardiac amyloidosis are predisposed to heart failure and arrhythmia, such as atrial fibrillation/flutter [2], and ATTRwt cardiac amyloidosis is the most common type of cardiac amyloidosis [3].

Histopathological demonstration of ATTR deposits in the tissue via endomyocardial biopsy is the gold standard for the diagnosis of ATTRwt cardiac amyloidosis; however, bone-avid radionuclide scintigraphy with comprehensive biochemical tests for a monoclonal gammopathy can reliably diagnose ATTRwt cardiac amyloidosis without the requirement of a biopsy [4]. Endomyocardial biopsy requires technical expertise. Moreover, although rare, it can cause severe complications associated with the procedure, such as cardiac tamponade and arrhythmias [5]. Sampling of alternative tissues has minimized its use. The feasibility of technetium-99m-labeled pyrophosphate (^{99m}Tc-PYP) imaging-based computed tomography (CT)-guided core-needle biopsy of the internal oblique muscle with tracer uptake as an extracardiac screening biopsy to confirm the presence of ATTR deposition in patients with ATTRwt cardiac amyloidosis has been reported [6]. Thirteen of the 18 patients (mean age, 86.3 years) included in this previous study were receiving one or 2 anticoagulants or/and antiplatelet agents. However, significant complications, such as the occurrence of intramuscular hematoma, were not observed with the use of this technique. This case report presents the case of a patient who developed an iatrogenic intramuscular hematoma of the external and internal oblique muscle after undergoing ^{99m}Tc-PYP imaging-based CT-guided core-needle biopsy of the internal oblique muscle to confirm the diagnosis of ATTR cardiac amyloidosis while receiving triple anti-thrombotic therapy for atrial flutter and coronary stenting.

Case presentation

A 73-year-old Japanese man (height, 170.7 cm; body weight, 83.0 kg) was transported via ambulance to the Yawatahama City General Hospital owing to dyspnea at rest, which developed suddenly 30 min prior. The patient had been smoking 30 cigarettes a day for 50 years but had no history of alcohol consumption. He was diagnosed with complex regional pain syndrome and underwent implantation of a spinal cord stimula-

Table 1 – Laboratory test results on admission.

Blood test parameter	Result	Reference value
C-reactive protein (mg/dL)	0.99	≤ 0.7
Total protein (g/dL)	9.1	6.7-8.3
Albumin (g/dL)	4.2	3.8-5.3
Total bilirubin (mg/dL)	0.7	0.2-1.2
ALT (IU/L)	12	≤ 40
AST (IU/L)	27	≤ 37
LDH (IU/L)	346	124-222
Alkaline phosphatase	112	38-113
Creatine kinase (U/L)	114	≤ 190
hs-cTnI (pg/mL)	35.8	≤ 18.4
BNP (pg/mL)	266.5	≤ 18.4
LDL cholesterol (mg/dL)	118	≤ 140
HDL cholesterol (mg/dL)	55	35-70
Triglyceride (mg/dL)	112	Fasting: 45-150
Glucose (mg/dL)	139	Fasting: 70-109
Glycated hemoglobin A1c (%)	6.0	4.6-6.2
Creatinine (mg/dL)	0.8	0.5-1.2
eGFR (mL/min per 1.73 m^2)	72	90-120
White blood cell (/μL)	11,300	4,000-8,500
Red blood cell (/μL)	451×10^4	400×10^4-550×10^4
Hemoglobin (g/dL)	14.5	13.0-17.5
Platelet (/μL)	28.6×10^4	14×10^4-40×10^4
APTT (sec)	24.5	23-40
Prothrombin time (sec)	10.4	10-13
D-dimer (μg/mL)	1.8	≤ 1.0
Free T3 (pg/mL)	3.42	2.52-4.06
Free T4 (ng/dL)	1.07	0.75-1.45
TSH (μIU mL)	5.7260	0.61-4.23

ALT, alanine aminotransferase; APTT, activated partial thromboplastin time; AST, aspartate aminotransferase; BNP, brain natriuretic peptide; eGFR, estimated glomerular filtration rate; HDL, high-density lipoprotein; hs-cTnI, high-sensitivity cardiac troponin I; LDH, lactate dehydrogenase; LDL, low-density lipoprotein; TSH, thyroid stimulating hormone.
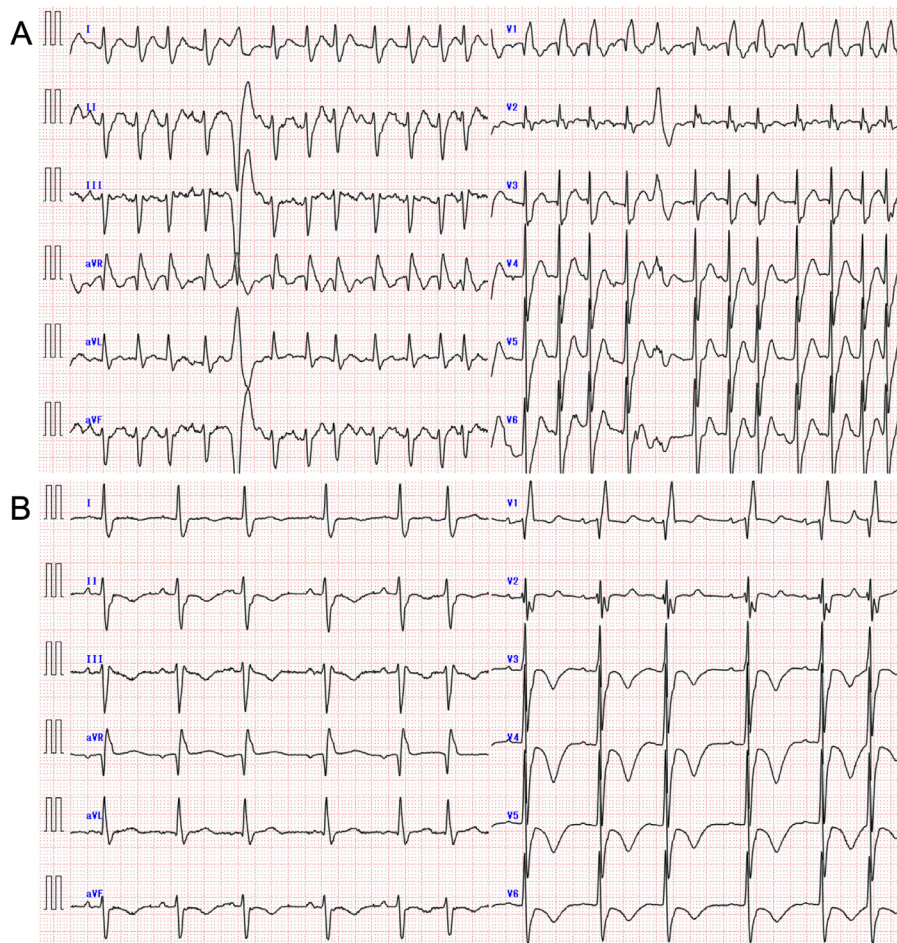
Fig. 1 – Electrocardiograms acquired on admission (A) and 30 hours (C) after first presentation. Panel A shows tachycardic atrial flutter with flutter waves at a rate of 300/min (cycle length, 200 ms) and an irregular ventricular rate of 151 beats/min, premature ventricular contraction, left axis deviation, and complete right bundle branch block. Panel B shows sinus rhythm with heart rate of 68 beats/min, premature atrial contractions, left axis deviation, complete right bundle branch block, ST-T abnormality, and QT prolongation with corrected QT-interval of 626 msec.

tor consisting of a pulse generator placed under the skin of left abdomen and stimulation electrodes located at the epidural space of the lower cervical level at another hospital 16 years prior. He had also undergone surgery for lumber spinal canal stenosis at the same hospital 3 years prior and was prescribed pregabalin (150 mg/day), tramadol hydrochloride (75 mg/day), acetaminophen (650 mg/day), amitriptyline hydrochloride (20 mg/day), and baclofen (10 mg/day) from the Department of Orthopedics, Yawatahama City General Hospital.

Physical examination on admission revealed a body temperature of 36.5°C, a pulse rate of 166 beats/min with an irregular rhythm, a systemic blood pressure of 259/179 mmHg, and a respiratory rate of 25 breaths/min, with oxygen saturation of 64% on room air measured using a pulse oximeter. No heart murmurs were audible upon auscultation; however, wet rales were detected in the lung fields. The liver and kidneys were not palpable. No pretibial edema was noted. Blood tests revealed elevated concentrations of high-sensitivity cardiac troponin I and brain natriuretic peptide (Table 1). Blood tests performed to evaluate the risk of coronary artery dis-

ease revealed normal lipid profiles but slightly elevated glucose levels. Chest radiography revealed pulmonary congestion. An electrocardiogram revealed tachycardic atrial flutter with a heart rate of 151 beats/min (Fig. 1A). A transthoracic echocardiogram showed diffusely hypokinetic wall motions in the left ventricle (LV) with a visually assessed ejection fraction (EF) of 20%. Thus, the patient was diagnosed with acute decompensated heart failure (ADHF) of Clinical Scenario class 1 caused by left ventricular systolic dysfunction, tachycardiac atrial flutter, and marked hypertension.

Oral edoxaban tosylate hydrate (60 mg/day) was administered to prevent cardiogenic thromboembolism (Table 2). Daily intravenous injections of furosemide (20 mg/day), continuous intravenous infusion of nitroglycerin, oral imidapril hydrochloride (5 mg/day), oral spironolactone (12.5 mg/day), and oral dapagliflozin propylene glycolate hydrate (10 mg/day) were administered for ADHF. Intravenous injection of nicardipine hydrochloride was administered for hypertensive emergency, and continuous intravenous infusion of landiolol hydrochloride (starting at 1 μg/kg/min and

Table 2 – Timeline of presentation.

Timeline	Patient history and test results	Treatment with anti-thrombotic agents
3 years prior to admission	The patient underwent surgery for lumber spinal canal stenosis.	
Day 1	The patient presented with acute onset of dyspnea. Chest radiography confirmed pulmonary congestion. ECG confirmed AF with HR of 151 beats/min. Echo confirmed LV dysfunction with visually estimated EF of 20%.	Administration of edoxaban tosilate hydrate initiated at a dose of 60 mg daily.
Day 2	ECG confirmed conversion to sinus rhythm.	
Day 8	Coronary CT confirmed moderate stenosis in the proximal LAD.	
Day 12	Follow-up Echo confirmed a reduced LV systolic function with an increase in the thickness of the wall and apical sparing.	
Day 15	CAG confirmed 75% stenosis at the proximal LAD with iFR of 0.74. A coronary stent was successfully deployed to the lesion with no residual stenosis.	Administration of prasugrel hydrochloride and aspirin initiated orally as single loading doses of 20 mg and 324 mg, respectively, just before PCI.
Day 16	^{99m}Tc-PYP SPECT confirmed abnormal tracer uptake into the myocardium and IOM. Subcutaneous abdominal fat pad fine-needle aspiration biopsy revealed no amyloid deposition.	Administration of prasugrel hydrochloride and aspirin was initiated at maintenance doses of 3.75 mg and 100 mg daily, respectively.
Day 19	^{99m}Tc-PYP imaging-based CT-guided core-needle biopsy of the IOM confirmed ATTR deposition.	
Day 20	The patient was discharged home.	

^{99m}Tc-PYP, technetium-99m-labeled pyrophosphate; AF, atrial flutter; ATTR, amyloid transthyretin; CAG, coronary angiography; CT, computed tomography; ECG, electrocardiogram; Echo, echocardiography; EF, ejection fraction; HR, heart rate; iFR, instantaneous wave-free ratio; IOM, internal oblique muscle; LAD, left anterior descending coronary artery; LV, left ventricular; PCI, percutaneous coronary intervention; SPECT, single photon emission computed tomography.

increasing to 5 μg/kg/min) was initiated to control the atrial flutter rate. The patient also received oxygen via a mask; however, his respiratory status did not improve sufficiently. Consequently, mechanical ventilatory support was initiated with nasal-biphasic positive airway pressure. In addition, continuous intravenous infusion of amiodarone hydrochloride was initiated to restore atrial flutter to sinus rhythm at an initial dose of 300 mg over the first 6 h and at a maintenance dose of 600 mg/day after the first 6 hours.

Atrial flutter converted to sinus rhythm (Fig. 1B) on day 2 of hospitalization, and an improvement in pulmonary congestion was observed. Therefore, the patient was weaned off the mechanical ventilator. Stepwise dose reductions were implemented on day 3 of hospitalization for the continuous intravenous infusion of landiolol hydrochloride and eventually discontinued. Oral administration of carvedilol was initiated for the left ventricular systolic dysfunction at an initial dose of 5 mg/day for week 1 based on his heart rate. The dosage was subsequently increased to 10 mg/day for week 2 and then to a dose of 15 mg/day for week 3. Continuous intravenous infusion of amiodarone hydrochloride was discontinued, and its oral administration was initiated on day 4.

Coronary CT angiography performed on day 8 of hospitalization revealed moderate stenosis in the proximal left anterior descending artery (LAD). A follow-up echocardiogram performed on day 12 of hospitalization demonstrated a reduction in the LV systolic function with an increase in the thickening of the wall and apical sparing (Fig. 2). Cardiac amyloidosis was suspected. Monoclonal protein studies using immunofixation electrophoresis of serum and urine and serum-free light chain

assays did not reveal plasma cell dyscrasia. Coronary angiography performed on day 15 of hospitalization via radial vascular access confirmed a moderate stenosis in the proximal LAD (Fig. 3). The instantaneous wave-free ratio in the LAD obtained with the use of a coronary-pressure guidewire was 0.74; thus, the patient was diagnosed with silent myocardial ischemia in the LAD. An intravascular ultrasonography-guided everolimus-eluting platinum chromium coronary stent was successfully deployed to the lesion without residual stenosis after administering loading doses of 20 mg and 324 mg of prasugrel hydrochloride and aspirin, respectively. Prasugrel hydrochloride and aspirin were continued at maintenance doses of 3.75 mg/day and 100 mg/day [7–9], respectively, on the next day.

On day 16 of hospitalization, ^{99m}Tc-PYP scintigraphy revealed tracer uptake in the myocardium and internal oblique muscles (Fig. 4). Fine-needle aspiration biopsy of the subcutaneous abdominal fat pad was performed in the usual manner on the same day; however, bleeding from the puncture site was greater than usual, necessitating compression for a long time [10]. Fine-needle aspiration biopsy did not reveal amyloid deposition.

On day 19 of hospitalization, ^{99m}Tc-PYP imaging-based CT-guided core-needle biopsy of the right abdominal internal oblique muscle was performed using a spring-loaded biopsy needle while receiving triple anti-thrombotic therapy (Figs. 5A-F) as described previously [6]. Immediately after obtaining 4 muscle fragments of approximately ≥1 mm^3 in size, approximately 29 min after commencing the procedure, blood began to trickle out of the biopsy needle. The needle was re-
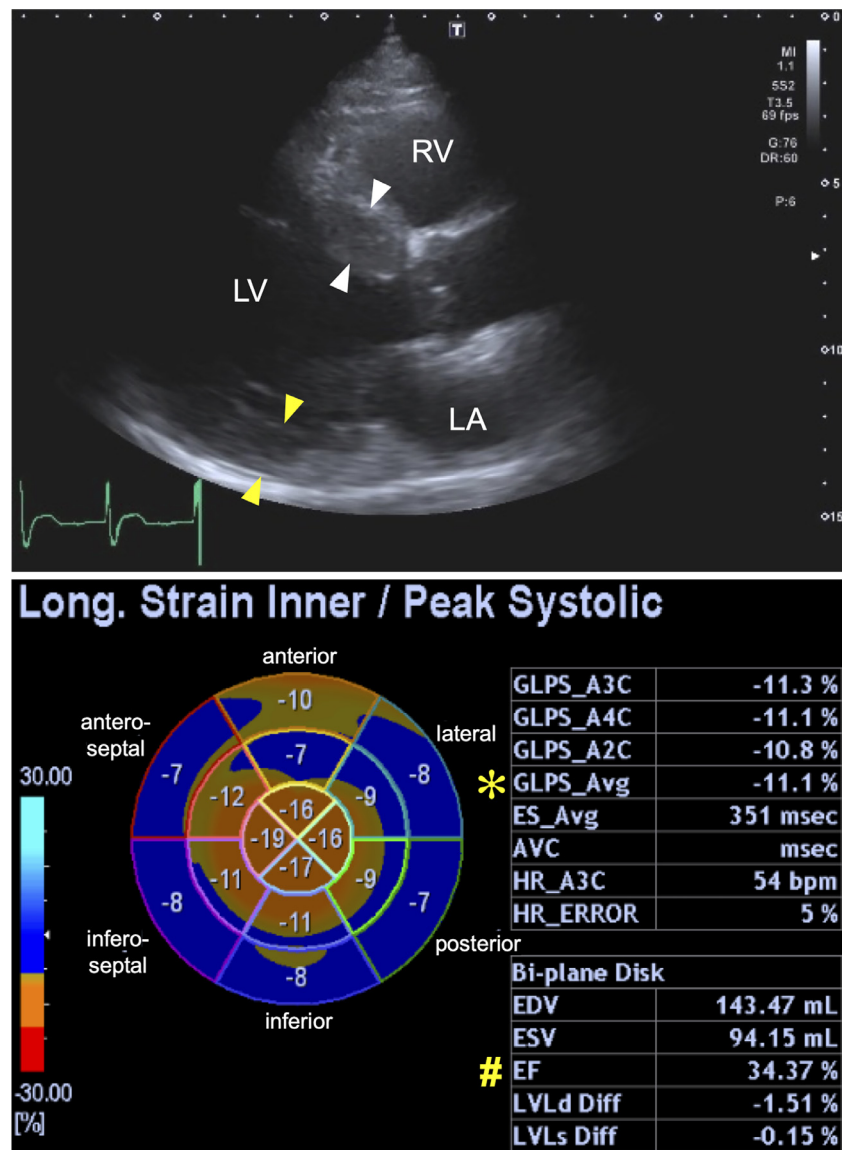
Fig. 2 – Transthoracic echocardiogram acquired on day 12 of hospitalization. A dilated left ventricle with an end-diastolic dimension of 57.0 mm, increase in the interventricular septum (white arrowheads) and left ventricular (LV) posterior wall (yellow arrowheads) of 14.2 mm and 14.4 mm, respectively, and normal-sized left atrium with a volume of 28.5 mL/m^2 are shown (upper panel). The bull's eye map (with the apex at the center of the color-coding map) illustrates segmental longitudinal LV peak systolic strain values of the 16-segment model generated by speckle-tracking analysis of 2-dimensional LV images acquired from the apical 2-, 3-, and 4-chamber views (A2C, A3C, and A4C, respectively) and shows a reduced LV ejection fraction (EF) of 34.4% (marked with a hash mark) and LV global longitudinal peak systolic strain (GLS) value, calculated as the mean of these 16 values, of -11.1% (marked with an asterisk) with an apical-to-basal strain ratio, calculated as apical septal longitudinal strain divided by average basal septal (anteroseptal and inferoseptal) longitudinal strain, of 2.5, indicating apical sparing (>2.1) (lower panel). LA, left atrium; LV, left ventricle; RV, right ventricle.

tracted immediately. CT revealed the development of an intramuscular hematoma involving the right external and internal oblique muscles. Manual compression hemostasis was initiated, and hemostasis was completed after confirming that the size of the hematoma had not increased on CT. The procedure duration, defined as the duration between the positioning of the patient on the scanner table and the end of the final CT acquisition, was 60 min. The dose-length product and effective dose were 253.2 mGy·cm and 5.1 mSv, respectively. The patient did not report pain in the right lateral abdomen thereafter. CT performed on day 20 of hospitalization revealed no expansion of the intramuscular hematoma (Fig. 5G), and the patient was discharged.

Congo red staining and immunohistochemical staining performed at Kumamoto University, a specialized amyloid center in Japan confirmed ATTR deposition in the tissue samples obtained via ^{99m}Tc-PYP imaging-based CT-guided core-needle biopsy of the right abdominal internal oblique muscle
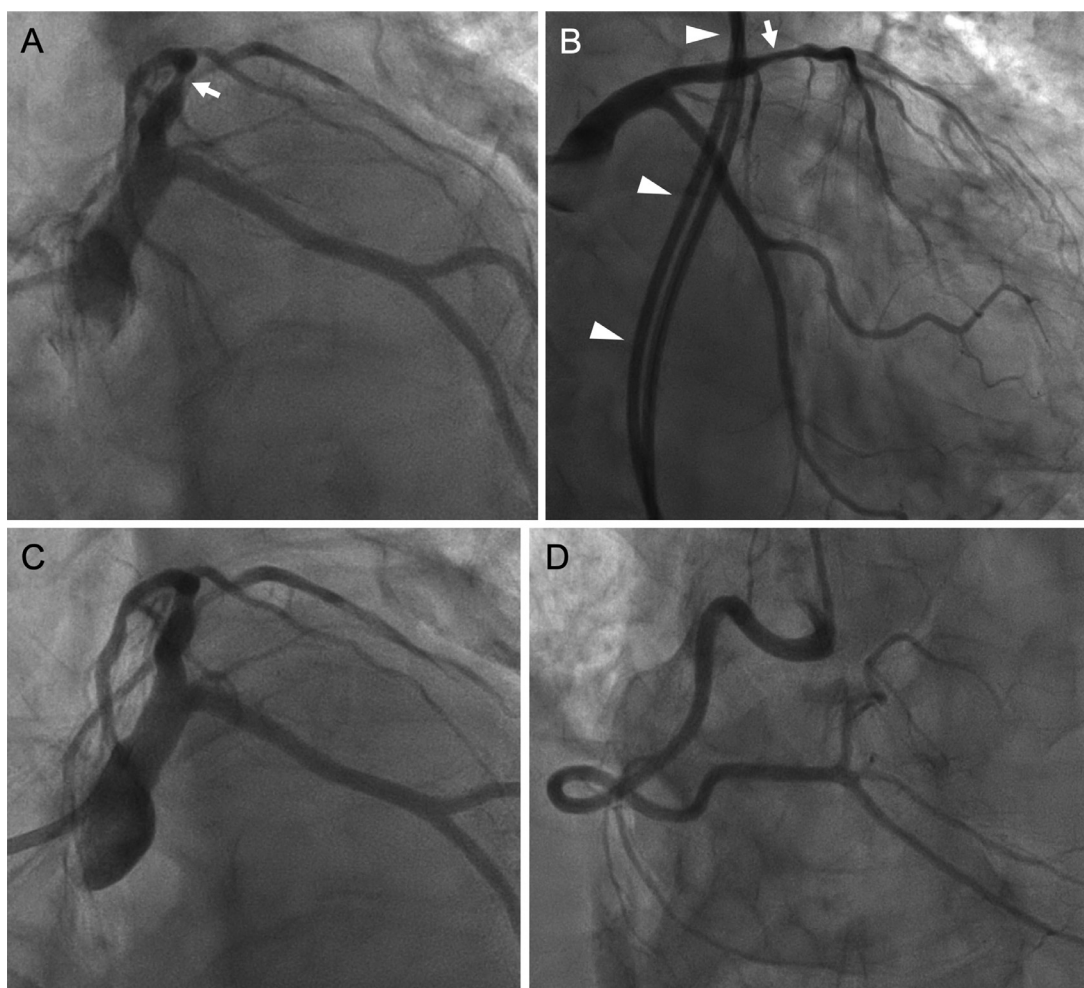
Fig. 3 – Coronary angiograms performed on day 15 of hospitalization. Moderate stenosis in the proximal left anterior descending artery (white arrows), but no significant stenosis in the right coronary artery or left circumflex coronary artery can be observed (Panels A, B, and D). An intravascular ultrasonography-guided 2.5 x 24 mm everolimus-eluting platinum chromium coronary stent was successfully deployed to the lesion and was post-dilated using a 3.0 mm non-compliant balloon without residual stenosis (Panel C). Final intravascular ultrasonography demonstrated good stent expansion and apposition without any complications, such as residual dissection (not illustrated). The images in panels A and C represent the 40° left anterior oblique and 30° caudal views, the image in panel B represents the anteroposterior and 30° caudal view, and the image in panel D represents the anteroposterior and 30° cranial view. White arrowheads indicate the leads of spinal cord stimulator.

(Fig. 6). TTR gene sequence testing indicated no variant; thus, the patient was diagnosed with ATTRwt amyloidosis and prescribed tafamidis. Ecchymosis on the right anterior and lateral abdomen associated with subcutaneous abdominal fat pad fine-needle aspiration biopsy and ^{99m}Tc-PYP imaging-based CT-guided internal oblique muscle biopsy was observed. However, they resolved spontaneously (Fig. 7). The time course regarding patient history, test results, and treatment with anti-thrombotic agents is shown in Table 2.

Discussion

Spontaneous hematomas of the external/internal oblique muscle are observed very rare, although hematomas can be associated with other conditions, such as abdominal trauma or iatrogenic injuries. These are classified according to CT findings [11,12]: type 1 is a mild intramuscular hematoma with a slight extension into the muscle, type 2 is a moderate intramuscular hematoma with bleeding observed between the abdominal internal oblique muscle and the transversalis fascia, and type 3 is a severe intramuscular hematoma that extends to the peritoneum. This case report presents the case of a patient receiving triple anti-thrombotic therapy for atrial flutter and coronary stenting who underwent ^{99m}Tc-PYP imaging-based CT-guided core-needle biopsy of the internal oblique muscle to confirm the diagnosis of ATTR cardiac amyloidosis. A type 1 intramuscular hematoma involving the external and internal oblique muscles developed subsequently; however, manual compression hemostasis prevented further increase in size.
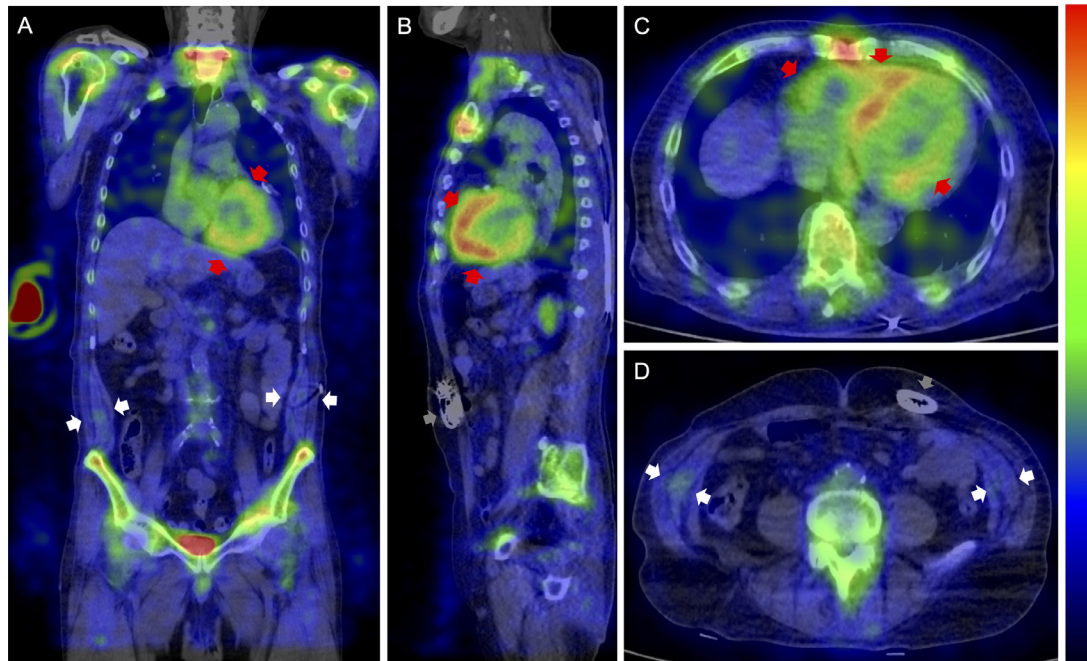
Fig. 4 – Chest- and abdomen-centered single-photon emission computed tomography/computed tomography fusion images of technetium-99m-labeled pyrophosphate (^{99m}Tc-PYP) scintigrams obtained 2 hours after injecting the radiotracer. Images show the (A) coronal plane, (B) sagittal plane, and horizontal plane of the (C) heart and (D) abdomen. The red and white arrows indicate the uptake of ^{99m}Tc-PYP in the myocardium and internal oblique muscles, respectively.

Extracardiac ^{99m}Tc-PYP uptake, which is detected in patients with ATTRwt cardiac amyloidosis, indicates the deposition of amyloid [10,13,14]. CT-guided core-needle biopsy of the internal oblique muscle with the highest uptake rate among the 11 skeletal trunk muscles studied [15] revealed a high amyloid detection rate without the incidence of significant complications, such as intramuscular hematoma identified on CT images, even when one or 2 antiplatelet or/and anticoagulant medications were not discontinued [6]. The internal oblique muscle is richly vascularized by 3 distinct arterial systems, namely, the ascending branch of the deep circumflex iliac artery, the lower 6 posterior intercostal arteries, and the lateral branches of the deep inferior epigastric artery [16]. The ascending branch of the deep circumflex iliac artery supplies a mean vascular territory of 35.7% of the internal oblique muscle. The lower 6 posterior intercostal arteries supply a mean vascular territory of 48.5%, whereas the lateral branches of the deep inferior epigastric artery supply a mean vascular territory of 15.8%. In contrast, the external oblique muscle derives its segmental arterial supply from the lower 6 or 7 posterior intercostal arteries. In addition, the muscular branches of the deep circumflex iliac artery also supply the lower part of the lowest one or 2 digitations. The areas of the vascular territories supplied by individual intercostal arteries vary from 9% to 22%. The percentages of individual vascular territories tend to become larger from the upper digitation to the lower digitation. The area of the vascular territory of the muscular branch of the deep circumflex iliac artery ranges from 5% to 18%. Thus, the external and internal abdominal oblique muscles lateral to the umbilical level, which

was the puncture site in this patient, might be the perfusion zone of the inferior intercostal arteries. The lower 6 posterior intercostal arteries course obliquely downward and medially in the plane between the internal oblique and transversus abdominis muscles to supply both muscles. These vessels vary between 0.5 and 1.0 mm in diameter and supply the upper portion of the internal oblique muscle segmentally. The branches pass through the internal oblique muscle to reach the external oblique muscle.

Atrial fibrillation or flutter is observed in 50%-60% of patients with ATTRwt cardiac amyloidosis [10,15,17,18]. Patients with cardiac amyloidosis are highly susceptible to atrial fibrillation/flutter-induced embolism [17,19]. In contrast, concomitant coronary artery disease occurs in 10%-20% of patients with ATTRwt cardiac amyloidosis [10,15,18,20]. Patients with atrial fibrillation/flutter require oral anticoagulation (OAC) for the prevention of cardiac thromboembolism, whereas patients undergoing percutaneous coronary intervention (PCI) require dual antiplatelet therapy (DAPT) with aspirin and P2Y$_{12}$ receptor inhibitor for the prevention of coronary thrombotic complications [9,21]. Patients with atrial fibrillation/flutter undergoing coronary stenting require a combination of OAC and DAPT, known as triple anti-thrombotic therapy, albeit for a short period of time. Triple anti-thrombotic therapy substantially increases the risk of bleeding. The latest guidelines advocate regimens that reduce the duration of triple anti-thrombotic therapy to 1 or 2 weeks; however, this decision must be made in consideration of bleeding and thrombotic risks in individual patients [9,21]. In addition, patients should discontinue P2Y$_{12}$ inhibitor and receive anti-
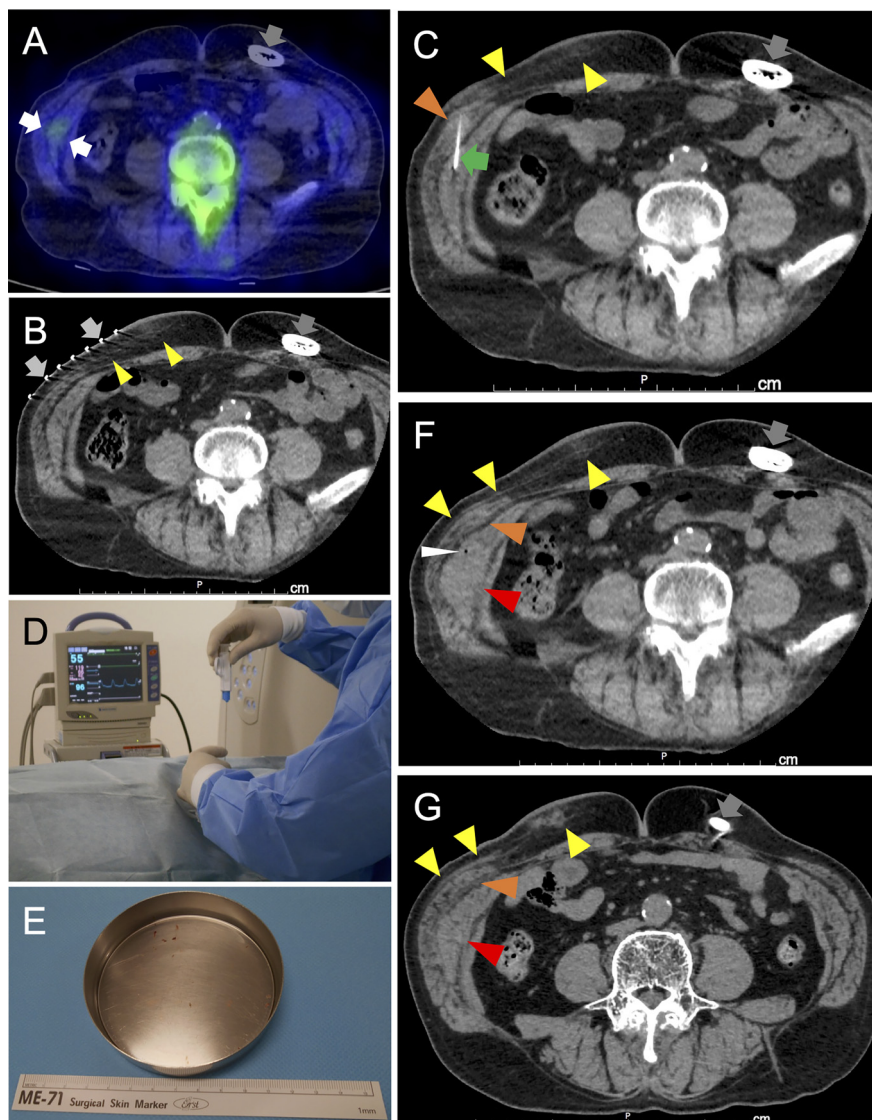
Fig. 5 – Technetium-99m-labeled pyrophosphate (⁹⁹ᵐTc-PYP) imaging-based computed tomography (CT)-guided core-needle biopsy of the right internal oblique muscle. The target site of the biopsy was the site with the highest ⁹⁹ᵐTc-PYP uptake in the right internal oblique muscle (white arrows) (A). The patient was positioned in the supine position on the CT scanner table, and the first CT images were obtained after applying the Guidelines® CT biopsy grid (Beekley Medical, Connecticut, United States) to the skin of the biopsy site to optimize the entry site of biopsy needle and improve first-stick accuracy (B, light gray arrows). After cleansing the biopsy site with an iodine solution, the skin, subcutaneous fat tissue, and fascia of the right oblique muscles were anesthetized with 0.5% procaine hydrochloride. A set of introducer stylet and cannula of the 18-gauge Fine Core® (Dr. Japan Corporation, Tokyo, Japan) spring-loaded semi-automatic biopsy needle with a length of 10 cm were advanced into the right internal oblique muscle through a small pre-incision of the skin. After confirming the correct orientation and depth on the CT images acquired subsequently (C), the introducer stylet was retracted, and the biopsy needle was advanced into the cannula left in place (D). A small intramuscular hematoma of the external oblique muscle developed during this time (orange arrowhead). Tissue sampling was then repeated with rotation of the cannula/needle at the same depth as well as at different depths, and immediately after obtaining 4 muscle fragments of approximately ≥1 mm³ in size (E), blood began to trickle out of the biopsy needle, which was approximately 29 min after commencing the procedure. The biopsy needle and introducer cannula were retracted immediately. CT image shows a Type 1 intramuscular hematoma of the right internal oblique muscles (red arrowheads) in addition to the hematoma of the external oblique muscle (orange arrowhead) (F). CT image acquired the day after ⁹⁹ᵐTc-PYP imaging-based CT-guided core-needle biopsy of the right internal oblique muscle shows a decrease in size of the intramuscular hematomas of the external and internal oblique muscles (G). Yellow arrowheads indicate the bleeding in the subcutaneous abdominal fat associated with the biopsy of the region. White arrowhead indicates air in the right internal oblique muscle occurred by the biopsy. Dark gray arrows indicate the pulse generator of the spinal cord stimulator placed under the skin of left abdomen.
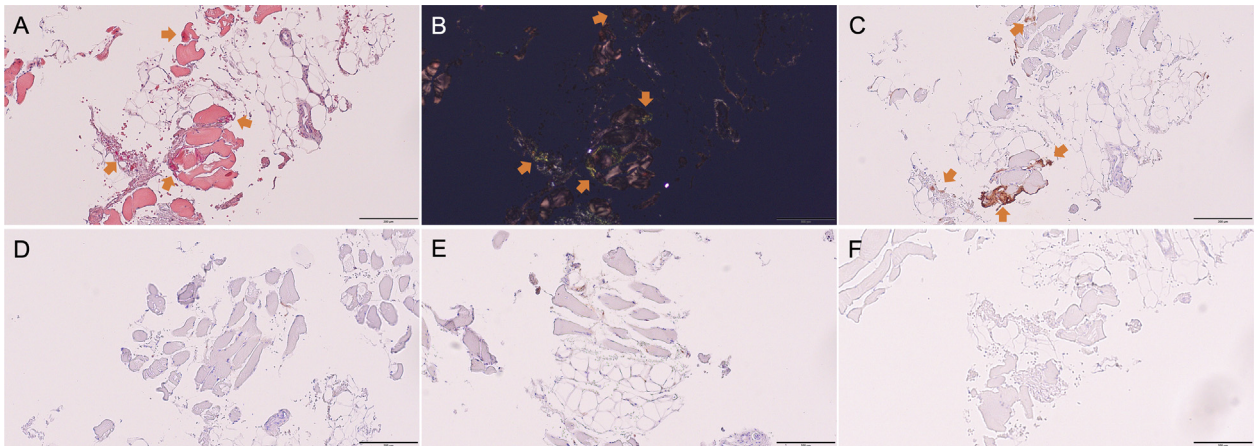
Fig. 6 – Histopathological images of computed tomography-guided core-needle biopsy of the right internal oblique muscle. The biopsy confirmed the presence of amyloid transthyretin in the muscle specimens obtained (orange arrows): red-orange under a light microscope (A) and apple-green birefringence under a cross-polarized light microscope (B) via Congo red staining; the positive result for the antibody raised against the anti-transthyretin 115-124 (polyclonal rabbit anti-human prealbumin, custom made) (C) and negative results for the antibodies raised against other amyloid proteins, anti-kappa light chain 116-133 (polyclonal rabbit anti-human kappa light chains, custom made) (D), anti-lambda light chain 118-134 (polyclonal rabbit anti-human lambda light chains, custom made) (E), and anti-amyloid A (monoclonal mouse anti-human amyloid A, DAKO) (F). The scale bars in all panels indicate 200 μm.

Fig. 7 – Ecchymosis on the right anterior and lateral abdomen 6 days after the subcutaneous abdominal fat pad fine-needle aspiration biopsy and 4 days after technetium-99m-labeled pyrophosphate (^{99m}Tc-PYP) imaging-based computed tomography (CT)-guided internal oblique muscle biopsy, respectively. Ecchymosis associated with subcutaneous abdominal fat pad fine-needle aspiration biopsy is more pronounced than that associated with ^{99m}Tc-PYP imaging-based CT-guided internal oblique muscle biopsy. The yellow arrow and ellipse in yellow dotted line indicate the puncture site of the skin and direction in which the 18-gauge Fine Core® (Dr. Japan Corporation, Tokyo, Japan) spring-loaded semi-automatic biopsy needle with a length of 10 cm was advanced into the right internal oblique muscle during ^{99m}Tc-PYP imaging-based CT-guided biopsy of the muscle, respectively. The white arrow and ellipse in white dotted line indicate the puncture site of the skin and direction in which an 18-gause needle with a length of 38 mm was advanced into the subcutaneous abdominal fat pad during the fine-needle aspiration biopsy of the region, respectively. The black arrowhead indicates the umbilicus.

thrombotic monotherapy with an anticoagulant alone following double anti-thrombotic therapy with an anticoagulant and P2Y$_{12}$ inhibitor for 6-12 months, depending on whether PCI is performed for acute or chronic coronary syndromes and the procedural complexity of PCI [21]. In this patient, co-administration of amiodarone, which inhibits P-glycoprotein, with edoxaban increased the peak and total exposure to edoxaban [22]. The recommended dose of edoxaban for Japanese patients weighing >60 kg and with creatinine clearance >50 mL/min is 60 mg. The present patient had a body weight of 83 kg, and the creatinine clearance calculated using the Cockcroft-Gault formula was 97 mL/min. However, the recommended dose of edoxaban should be reduced to 30 mg when amiodarone and edoxaban are used together. Non-vitamin K antagonist oral anticoagulant (NOAC) including edoxaban should be preferred over vitamin K antagonist; however, the dose must be reduced in accordance with the label criteria.

A previous study wherein 18 patients with ATTRwt cardiac amyloidosis were enrolled revealed that ^{99m}Tc-PYP imaging-based CT-guided core-needle biopsy of the internal oblique muscle seems to be safe with no complications, such as bleeding, observed. However, it must be noted that internal oblique hematoma can occur even as a result of non-traumatic injuries, such as overcontraction or overstretching of the abdominal muscles due to coughing, sneezing, twisting, or vomiting, in rare cases [11]. Biopsies can cause major bleeding, especially in elderly patients who are unable to rest during the procedure due to cognitive impairment or pain in the back or extremities [23]. This is particularly observed in patients with risk factors, such as anticoagulation, coagulopathies, and end-stage renal disease [24]. The biopsy for ATTRwt cardiac amyloidosis targets elderly patients who are at considerable risk of bleeding due to factors such as multimorbidity, polypharmacy, frailty/dementia, and decreased renal function [10,15,20]; thus, efforts should be made to reduce the incidence of complications, such as delaying the procedure until the dosage of at least one antithrombotic drug can be reduced or skipping one dose of anti-thrombotic medication. In the case of NOAC, which has a rapid onset and offset of action, the timing of discontinuation of the drug, the type of drug, and the renal function of the patient should be taken into account when scheduling the procedure to minimize the duration of treatment interruption. Nonetheless, as in the present case, the hematoma can be detected fairly quickly, and immediate treatments, such as compression hemostasis, can prevent the hematoma from expanding. Endovascular treatment must be performed if hemostasis cannot be achieved and the hematoma enlarges; however, the possibility of the incidence of this complication is very low.

Conclusions

We present the case of a patient receiving triple anti-thrombotic therapy for atrial flutter and coronary stenting who underwent ^{99m}Tc-PYP imaging-based CT-guided core-needle biopsy of the internal oblique muscle owing to suspected ATTR cardiac amyloidosis. Type 1 intramuscular hematoma of the external and internal oblique muscles developed subsequently; however, compression hemostasis prevented any further increase in size. Since this biopsy is often performed in patients at high risk of bleeding owing to factors such as advanced age, multimorbidity, and polypharmacy, measures should be taken to reduce the incidence of bleeding complications.

Patient consent

Written informed consent was obtained from the patient and his family for the procedure and publication of this report and any accompanying images.

REFERENCES

[1] Bezerra F, Saraiva MJ, Almeida MR. Modulation of the mechanisms driving transthyretin amyloidosis. Front Mol Neurosci 2020;13:592644. doi:10.3389/fnmol.2020.592644.

[2] Giancaterino S, Urey MA, Darden D, Hsu JC. Management of arrhythmias in cardiac amyloidosis. JACC Clin Electrophysiol 2020;6(4):351–61. doi:10.1016/j.jacep.2020.01.004.

[3] Picken MM. The pathology of amyloidosis in classification: a review. Acta Haematol 2020;143(4):322–34. doi:10.1159/000506696.

[4] Rauf MU, Hawkins PN, Cappelli F, Perfetto F, Zampieri M, Argiro A, et al. Tc-99m labelled bone scintigraphy in suspected cardiac amyloidosis. Eur Heart J 2023;44(24):2187–98. doi:10.1093/eurheartj/ehad139.

[5] Porcari A, Baggio C, Fabris E, Merlo M, Bussani R, Perkan A, et al. Endomyocardial biopsy in the clinical context: current indications and challenging scenarios. Heart Fail Rev 2023;28(1):123–35. doi:10.1007/s10741-022-10247-5.

[6] Takahashi K, Hiratsuka Y, Iwamura T, Sasaki D, Yamamura N, Kitazawa S, et al. Technetium-99m-pyrophosphate imaging-based computed tomography-guided core-needle biopsy of internal oblique muscle in wild-type transthyretin cardiac amyloidosis. Amyloid 2023:1–10 Online ahead of print. doi:10.1080/13506129.2023.2235881.

[7] Lee CR, Luzum JA, Sangkuhl K, Gammal RS, Sabatine MS, Stein CM, et al. Clinical Pharmacogenetics Implementation Consortium guideline for CYP2C19 genotype and clopidogrel therapy: 2022 update. Clin Pharmacol Ther 2022;112(5):959–67. doi:10.1002/cpt.2526.

[8] Sawayama Y, Yamamoto T, Tomita Y, Asada K, Yagi N, Fukuyama M, et al. Comparison between clopidogrel and prasugrel associated with CYP2C19 genotypes in patients receiving percutaneous coronary intervention in a Japanese population. Circ J 2020;84(9):1575–81. doi:10.1253/circj.CJ-20-0254.

[9] Nakamura M, Kimura K, Kimura T, Ishihara M, Otsuka F, Kozuma K, et al. JCS 2020 guideline focused update on antithrombotic therapy in patients with coronary artery disease. Circ J 2020;84(5):831–65. doi:10.1253/circj.CJ-19-1109.

[10] Takahashi K, Sasaki D, Yamashita M, Sakaue T, Enomoto D, Morioka H, et al. Amyloid deposit corresponds to technetium-99m-pyrophosphate accumulation in abdominal fat of patients with transthyretin cardiac amyloidosis. J Nucl Cardiol 2022;29(6):3126–36. doi:10.1007/s12350-021-02890-6.

[11] Afşin E, Cosgun Z. A rare cough complication: internal oblique muscle hematoma. Radiol Case Rep 2021;16(5):1015–18. doi:10.1016/j.radcr.2021.01.059.

[12] Berná JD, Garcia-Medina V, Guirao J, Garcia-Medina J. Rectus sheath hematoma: diagnostic classification by CT. Abdom Imaging 1996;21(1):62–4. doi:10.1007/s002619900011.

[13] Takahashi K, Sasaki D, Sakaue T, Enomoto D, Uemura S, Okura T, et al. Extracardiac accumulation of technetium-99m-pyrophosphate in transthyretin cardiac amyloidosis. JACC Case Rep 2021;3(7):1069–74. doi:10.1016/j.jaccas.2021.02.015.

[14] Takahashi K, Morioka H, Sasaki D, Yamamura N, Kitazawa S, Ueda M, et al. Two autopsy cases of wild-type transthyretin cardiac amyloidosis who died 10 days after technetium-99m-pyrophosphate scintigraphy. J Nucl Cardiol 2022 Online ahead of print. doi:10.1007/s12350-022-03128-9.

[15] Takahashi K, Hiratsuka Y, Sasaki D, Sakaue T, Enomoto D, Morioka H, et al. ^{99m}Tc-pyrophosphate scintigraphy can image tracer uptake in skeletal trunk muscles of transthyretin cardiac amyloidosis. Clin Nucl Med 2023;48(1):18–24. doi:10.1097/RLU.0000000000004397.

[16] Yang D, Morris SF, Geddes CR, Tang M. Neurovascular territories of the external and internal oblique muscles. Plast Reconstr Surg 2003;112(6):1591–5. doi:10.1097/01.PRS.0000085819.74215.C0.

[17] Kitaoka H, Izumi C, Izumiya Y, Inomata T, Ueda M, Kubo T, et al. JCS 2020 guideline on diagnosis and treatment of cardiac amyloidosis. Circ J 2020;84(9):1610–71. doi:10.1253/circj.CJ-20-0110.

[18] González-López E, Gagliardi C, Dominguez F, Quarta CC, de Haro-Del Moral FJ, Milandri A, et al. Clinical characteristics of wild-type transthyretin cardiac amyloidosis: disproving myths. Eur Heart J 2017;38(24):1895–904. doi:10.1093/eurheartj/ehx043.

[19] Takahashi K, Yamashita M, Sakaue T, Enomoto D, Uemura S, Okura T, et al. Light chain cardiac amyloidosis in a nonagenarian. J Geriatr Cardiol 2022;19(1):83–9. doi:10.11909/j.issn.1671-5411.2022.01.008.

[20] Ochi Y, Kubo T, Baba Y, Sugiura K, Ueda M, Miyagawa K, et al. Wild-type transthyretin amyloidosis in female patients-consideration of sex differences. Circ Rep 2021;3(8):465–71. doi:10.1253/circrep.CR-21-0067.

[21] Angiolillo DJ, Bhatt DL, Cannon CP, Eikelboom JW, Gibson CM, Goodman SG, et al. Antithrombotic therapy in patients with atrial fibrillation treated with oral anticoagulation undergoing percutaneous coronary intervention: a north American perspective: 2021 update. Circulation 2021;143(6):583–96. doi:10.1161/CIRCULATIONAHA.120.050438.

[22] Parasrampuria DA, Truitt KE. Pharmacokinetics and pharmacodynamics of edoxaban, a non-vitamin K antagonist oral anticoagulant that inhibits clotting factor xa. Clin Pharmacokinet 2016;55(6):641–55. doi:10.1007/s40262-015-0342-7.

[23] Kennedy SA, Milovanovic L, Midia M. Major bleeding after percutaneous image-guided biopsies: frequency, predictors, and periprocedural management. Semin Intervent Radiol 2015;32(1):26–33. doi:10.1055/s-0034-1396961.

[24] Farrelly C, Fidelman N, Durack JC, Hagiwara E, Kerlan RK Jr. Transcatheter arterial embolization of spontaneous life-threatening extraperitoneal hemorrhage. J Vasc Interv Radiol 2011;22(10):1396–402. doi:10.1016/j.jvir.2011.06.008.